Original Article

JCBFM

Journal of Cerebral Blood Flow & Metabolism
2019, Vol. 39(10) 2048–2060

DOI: 10.1177/0271678X18777916
journals.sagepub.com/home/jcbfm
SAGE

Annexin A2 is a Robo4 ligand that modulates ARF6 activation-associated cerebral trans-endothelial permeability

Wenlu Li[1,2,3,*], Zhigang Chen[1,*], Jing Yuan[3], Zhanyang Yu[3], Chongjie Cheng[3], Qiuchen Zhao[3], Lena Huang[3], Katherine A Hajjar[4], Zhong Chen[2], Eng H Lo[3], Haibin Dai[1] and Xiaoying Wang[3]

Abstract

Blood–brain barrier (BBB) disruption in neurological disorders remains an intractable problem with limited therapeutic options. Here, we investigate whether the endothelial cell membrane protein annexin A2 (ANXA2) may play a role in reducing trans-endothelial permeability and maintaining cerebrovascular integrity after injury. Compared with wild-type mice, the expression of cerebral endothelial junctional proteins was reduced in E15.5 and adult ANXA2 knockout mice, along with increased leakage of small molecule tracers. In human brain endothelial cells that were damaged by hypoxia plus IL-1β, treatment with recombinant ANXA2 (rA2) rescued the expression of junctional proteins and decreased trans-endothelial permeability. These protective effects were mediated in part by interactions with F-actin and VE-cadherin, and the ability of rA2 to modulate signaling via the roundabout guidance receptor 4 (Robo4)-paxillin-ADP-ribosylation factor 6 (ARF6) pathway. Taken together, these observations suggest that ANXA2 may be associated with the maintenance of endothelial tightness after cerebrovascular injury. ANXA2-mediated pathways should be further explored as potential therapeutic targets for protecting the BBB in neurological disorders.

Keywords

Human brain microvascular endothelial cells, annexin A2, trans-endothelial permeability, junctional proteins, Robo4-paxillin-ARF6 signaling

Received 21 December 2017; Revised 3 April 2018; Accepted 24 April 2018

Introduction

The blood–brain barrier (BBB) is affected in almost all CNS disorders. There are many aspects to BBB dysfunction including alterations in adherens and tight junctions, transporter trafficking, upregulation of neurovascular proteases, and perturbations in cell–cell and cell–matrix signaling.[1–4] Hence, rescuing the damaged BBB is a challenging problem.

Although BBB function involves a complex web of interactions between multiple components in the neurovascular unit, the proper expression and distribution of junctional proteins between cerebral endothelial cells are often considered a first and essential requirement.[5,6] However, there are currently no viable therapeutic approaches to rescue the molecular regulation of junctional processes and protect the BBB.

[1]The Second Affiliated Hospital, Zhejiang University School of Medicine, Hangzhou, China
[2]College of Pharmaceutical Sciences, Zhejiang University, Hangzhou, China
[3]Neuroprotection Research Laboratory, Massachusetts General Hospital, Harvard Medical School, Charlestown, MA, USA
[4]Department of Cell and Developmental Biology, Weill Cornell Medical College, New York, NY, USA

*Co-first authors.

Corresponding authors:
Haibin Dai, the Second Affiliated Hospital, Zhejiang University School of Medicine, Hangzhou, Zhejiang 310009, China.
Email: haibindai@zju.edu.cn
Xiaoying Wang, Neuroprotection Research Laboratory, Massachusetts General Hospital, Harvard Medical School, Charlestown, MA 02129, USA.
Email: wangxi@helix.mgh.harvard.edu
Zhong Chen, College of Pharmaceutical Sciences, Zhejiang University, Hangzhou, Zhejiang 310058, China.
Email: chenzhong@zju.edu.cn

In peripheral endothelial cells, annexin A2 (ANXA2) is an F-actin cytoskeleton-binding protein that is involved in regulating tight junction formation.[7] In human umbilical vein endothelial cells, ANXA2 binds VE-cadherin and stabilizes adherent junctions.[8,9] In epithelial cells, ANXA2 has been proposed as a new class of membrane proteins that assist in tight junction assembly.[10] More recently, we found that ANXA2 helps maintain pulmonary microvascular integrity, and prevents vascular leak during alveolar hypoxia by enabling vascular endothelial cadherin-related phosphatase activity.[11] Based on these emerging findings in peripheral systems, we now hypothesize that ANXA2 may also be a key component of the cerebral endothelium that is involved in the maintenance of junctional integrity and BBB function.

In the present study, we used *Anxa2*$^{-/-}$ mice and a cell culture system to demonstrate that (1) ANXA2 plays a key role in the regulation of cerebral endothelial permeability under both physiological and hypoxic/inflammatory conditions, (2) ANXA2 function is mediated in part via F-actin-VE-cadherin and Robo4-paxillin-ADP-ribosylation factor 6 (ARF6) signaling, and (3) exogenous recombinant ANXA2 (rA2) decreases cerebral trans-endothelial permeability after hypoxia and inflammatory injury. Taken together, our observations indicate that ANXA2 might comprise a new therapeutic target for rescuing trans-endothelial tightness and BBB function after brain injury and CNS disease.

Materials and methods

In vivo BBB permeability assay

The BBB permeability assay for embryonic mice was based on previously described methods.[12,13] Briefly, E15.5 pregnant mice were deeply anesthetized with isoflurane. Using a Hamilton syringe, 5 µl of 10-kDa dextran-tetramethylrhodamine (lysine fixable, 4 mg ml^{-1}, D3312, Invitrogen) or 10 µl of EZ-link NHS-sulfobiotin (50 mg ml^{-1}, 21335, Thermo) was injected into the embryonic liver to minimize changes in blood pressure. The markers were allowed to circulate for 30 min before the animals were killed and the brains were removed. Injections of fluorescein-labeled lectin (10 mg/kg, FLK-2100, Vector Laboratories) were made through the tail vein to visualize cerebral microvessels. For adult mice, the two tracers were injected directly into the left ventricle of the heart. Brains were dissected and fixed by immersion in 4% PFA at 4°C overnight, cryopreserved in 30% sucrose and frozen in TissueTekOCT (Sakura). Sections of 12 µm thickness were collected, and BBB leakage was examined with fluorescence microscopy (Nikon ECLIPSE Ti-S, Japan). All experiments were performed following protocols approved by the Massachusetts General Hospital Institutional Animal Care and Use Committee in compliance with the NIH Guide for the Care and Use of Laboratory Animals and were in compliance with ARRIVE (Animal Research: Reporting In Vivo Experiments) guidelines. *Anxa2*$^{-/-}$ mice on the C57BL/6 background were generated as described previously.[14] Age-matched wild-type mice with the same strain background were used as controls. In this study, group sizes were derived from power calculations (alpha = 0.05, beta = 0.80) based on standard models, our previously published papers, or pilot data. All experiments were performed with allocation concealment, randomization, and blinding.

Production of recombinant human ANXA2 (rA2)

rA2 was produced as previously described.[15] Briefly, rA2 was expressed in an *Escherichia coli* batch fermentation process, starting from a research cell bank using Luria-Bertani-glucose medium with isopropyl β-D-1-thiogalactopyranoside induction. The soluble protein was purified using a combination of hydrophobic interaction chromatography, ion exchange chromatography, and hydroxyapatite chromatography, produced in the Bioexpression and Fermentation Facility at the University of Georgia (http://bff.uga.edu/). The final rA2 purity is 96% (endotoxin 0.5 EU/mg) with a concentration of 8 mg/ml.

Cell cultures

Primary human brain microvascular endothelial cells (HBMVEC) were purchased at passage 5 from Cell Systems and used at passages 7–10, as previously described.[16,17] Briefly, HBMVEC were cultured in flasks coated with rat tail collagen I (Corning, Bedford, MA) and maintained in endothelial basal medium (EBM)-2 (Lonza, Hopkinton, MA) supplemented with fetal bovine serum, fibroblast growth factor-2, epidermal endothelial growth factor, hydrocortisone, insulin-like growth factor, ascorbic acid, BEGF, and amphotericin B. HBMVEC were grown to about 100% confluence and then exposed to IL-1β (20 ng/ml) plus hypoxia which was induced by placing the cells in an air-tight chamber (Billups-Rothenberg) and perfusing the chamber with 90% N_2, 5% CO_2, and 5% H_2 for 30 min. The chamber was then sealed and kept at 37°C for 24 h.

Transfection with short interfering RNA

ANXA2 short interfering RNA (siRNA) (sc-270151, Santa Cruz Biotechnology) was diluted with Lipofectamine RNAiMAX (Invitrogen) and Opti-MEM (Invitrogen), and then incubated for 10 min at room

temperature. The siRNA was added in cell media (final concentration of siRNA was 10 nM). Treatments were repeated once every 3 days after the initial transfection.

In vitro trans-endothelial permeability assay

The standard horseradish peroxidase leakage assay was performed following previously described methods.[17,18] Briefly, HBMVEC were seeded on transwell PET membranes (0.4 μm pore, 11 mm diameter; Corning, Lowell, MA) at a density of 2.5×10^5 cells per membrane. The PET membrane was coated with collagen (15 μg/ml; 354236, Corning). Cells were grown to confluence and treated with 100 nM rA2 for 30 min followed by 24 h hypoxia plus 20 ng/ml IL-1β. To assess paracellular permeability, horseradish peroxidase (Sigma) was added into the luminal chamber at a concentration of 100 μg/ml in 500 μl media. After 1 h incubation, 0.5 mM of guaiacol (Sigma) and 0.6 mM H_2O_2 (Sigma) were added into the media obtained from lower (abluminal) chamber. Fluorescence intensity was measured with a fluorescence reader at 490 nm of absorbance. Paracellular permeability was calculated by measuring the diffusion of horseradish peroxidase from luminal to the abluminal chamber.[19]

Transendothelial electrical resistance

HBMVEC were seeded on transwell PET membranes (0.4 μm pore, 11 mm diameter; Corning) at a density of 2.5×10^5 cells per membrane. The PET membrane was coated with collagen (15 μg/ml; 354236, Corning). Cells were grown to confluence and treated with 100 nM rA2 for 30 min followed by 24 h hypoxia plus 20 ng/ml IL-1β. Transendothelial electrical resistance (TEER) was monitored using an Evometer (World Precision Instruments, FL) fitted with a Chopstick electrode. Results were normalized by the area of the monolayer, and the background TEER of blank inserts was subtracted from the TEER of the HBMVEC monolayer. Note: in this study, we found that absolute TEER values may be a bit below 100; slightly lower than some previously reported values in the literature.[9] This may be due to the specific settings of our equipment and cell culture density.

Quantitative polymerase chain reaction

Total RNA was extracted from cells or tissues using the RNeasy plus mini kit (Qiagen), and RNA was converted to cDNA using RETROscript kit as previously described.[20,21] Quantitative real-time polymerase chain reaction was performed using Taqman probes (zonula occludens-1 (*ZO1*), Hs01551861_m1, Mm00493699_m1; *VE-Cadherin*, Hs00901463, Mm00486938_m1; *Occludin*, Hs00170162_m1, Mm00500912_m1; *Claudin-5*, Hs00533949_s1, Mm00727012_s1; *GAPDH*, Hs02758991_g1, Mm03302249_g1), and samples were run on the ABI Prism 7500 HT Real-Time PCR system (Applied Biosystems).

Membrane fraction isolation

Plasma membrane and membrane-associated proteins were isolated following manufacturer's protocol (444810, Calbiochem, MA). Briefly, after treatment, the cell monolayer was washed two times with cold wash buffer. After washing, cells were added Protease Inhibitor Cocktail and cold Extraction Buffer I. Carefully mixed the components by swirling the flask without disturbing the monolayer. Cells were incubated for 10 min at 4°C under gentle agitation; then the supernatant was discarded. Cells were added Protease Inhibitor Cocktail and cold Extraction Buffer II. Carefully mixed the components by swirling the flask without disturbing the monolayer. Cells were incubated for 30 min at 4°C under gentle agitation, and the supernatant was saved as a soluble membrane fraction. Note: although this is a standard and commonly used method and the majority of the isolated membrane fraction should comprise external cellular membranes, these fractions may also include smaller portions of intracellular membranes. This is a caveat that should be kept in mind for data interpretation.

Immunocytochemistry

HBMVEC were seeded into 24-well plate coated with collagen. After growing into confluence, cells were treated with 100 nM rA2 or 10 μM SecinH3 for 30 min followed by 24 h hypoxia plus 20 ng/ml IL-1β. Cells were then washed with phosphate buffered saline (PBS) and fixed with 4% paraformaldehyde (PFA). After permeabilization with 0.5% Triton, the cells were blocked with normal donkey serum and stained with anti-VE-cadherin (Product number ALX-210-232-C100, Enzo) or ZO-1 (339100, Invitrogen), followed by 568/588 Alexa Fluor-conjugated or 488 Alexa Fluor-conjugated secondary antibodies (1:200–1:500), or with 488 Alexa Fluor phallodin to detect F-actin (Invitrogen). Slides were mounted in fluorescence gel (H-1200, Vector) and visualized by fluorescence, light, or confocal microscopy as previously described.[17,22]

Western blots

Western blots were performed following standard methods.[17,23] Pro-PREP Protein Extraction Solution (iNtRON Biotechnology) was used to collect samples. Protein levels of samples were determined by the BCA assay (5000201, Bio-Rad Laboratories, CA). Fifty

micrograms of protein samples were loaded onto 4–20% Tris-glycine gels. After electrophoresis and blotting onto polyvinylidene difluoride membranes, the membranes were blocked in Tris-buffered saline containing 5% nonfat milk for 60 min at room temperature. The membranes were then probed with primary antibodies against ZO-1 (96594, Abcam), VE-cadherin (33169, Abcam), Occludin (64482, Abcam), Claudin-5 (15106, Abcam), and Na^+K^+ATPase (198366, Abcam) at 4°C overnight. Horseradish peroxidase-conjugated secondary antibodies were then used at 25°C for 1 h. Signals were detected by chemiluminescence. Note: For VE-cadherin and Occludin western blots, there appear to be multiple bands, which is likely due to some limitations in antibody specificity (please see online Supplementary Data for the original blots).

Immunoprecipitation

The immunoprecipitation (IP) assay was performed following standard protocols (10007D, Invitrogen). Briefly, cells were washed with cold PBS and lysed with lysis buffer that contained protease inhibitors. Cell lysates were centrifuged, and the supernatants were saved. Protein concentration was determined by bovine serum albumin (BSA) assay (Bio-Rad). Dynabeads weighing 1.5 mg were incubated with antibodies for 10 min at room temperature with rotation. After washing, dynabeads were incubated with cell lysates obtained as above for 10 min at room temperature with rotation. After a second wash, target antigens were eluted using 20 µl elution buffer and 10 µl premixed LDS sample buffer and reducing agent. The immunoprecipitates were assessed by western blot analysis.

ARF6–GTP pull-down assay

The ARF6 Activation Assay Kit was used following standard protocols (STA-407-6, Cell Biolabs). Briefly, HBMVEC were treated with 100 nM rA2 for 30 min followed by 20 ng/ml IL-1β or hypoxia plus 20 ng/ml IL-1β. Additionally, the selective ARF6 activator 10 µM QS11 (ab141408, Abcam) or selective ARF6 inhibitor 30 µM SecinH3 (Calbiochem) were also used in combination with hypoxia plus 20 ng/ml IL-1β or 100 nM rA2 for 24 h. Cells were then washed with cold PBS. ARF6 pull-down lysis buffer and protease inhibitors were added to the cells. Cell lysates were centrifuged, and the supernatants were added to GGA3-conjugated beads, and then incubated at 4°C for 1 h with gentle agitation. Beads were washed in lysis buffer and resuspended in 2X reducing SDS–PAGE sample buffer. ARF6-GTP (Guanosine-5′-triphosphate)/Total ARF6 represented for quantification of relative ARF6 activity. A part of cell lysis was used as a measure of total ARF6. In this experiment, both ARF6 activator and inhibitor were applied according to previously published papers.[24,25] ARF–GAP inhibitor QS11 evokes an increase in ARF6–GTP of endothelial cells; therefore QS11 was selected as ARF6 activator.[24] SecinH3 is an inhibitor of cytohesin, which is a small guanine nucleotide exchange factor that stimulates ADP-ribosylation factors including ARF6. Thus, we used SecinH3 as ARF6 inhibitor.[24,25]

Statistical analysis

All data are expressed as mean ± SD. For parametric measurements, we used analysis of variance followed by Tukey–Kramer post hoc tests. For nonparametric ordinal data, we used nonparametric Kruskal–Wallis tests followed by post hoc Mann–Whitney tests. A *P*-value of less than 0.05 was considered statistically significant.

Results

ANXA2 gene knockout impairs BBB integrity

First, we investigated the function of ANXA2 in BBB development. In E15.5 embryos, the large 10 kDa dextran tracer was restricted within cortical microvessels in both *Anxa2*$^{-/-}$ and WT mice (Figure 1(a)). However, the smaller tracer sulfo-NHS-biotin (~550 Da) was detected outside cortical microvessels in the *Anxa2*$^{-/-}$ mice but not WT mice (Figure 1(b)). In adult *Anxa2*$^{-/-}$ mice, leakage of the small 550 Da tracer was reduced compared to the E15.5 embryos, but some signals still appeared to be detectable outside microvessels (Figure 1(c)). These data suggest that in *Anxa2*$^{-/-}$ mice, although the BBB may continue to develop, it takes place more slowly and in an incomplete way. In isolated cerebral microvessel (CMV) fragments, mRNA (Figure 1(d)) and protein (Figure 1(e)) expression levels of ZO-1, claudin-5, and VE-cadherin in adult male *Anxa2*$^{-/-}$ mice were all significantly reduced. Taken together, these observations suggest that ANXA2 may play a role in the development and regulation of primary cerebral endothelial junction proteins.

Role of ANXA2 in the regulation of trans-endothelial permeability after hypoxia plus IL-1β insult

Based on the in vivo observations, we asked whether ANXA2 played a role in the maintenance of cerebral endothelial integrity in vitro. Endogenous expression of ANXA2 was suppressed by siRNA (Figure 2(a)), and trans-endothelial permeability was quantified with a standard horseradish peroxidase assay. Compared to scrambled siRNA control (Con), suppression of endogenous ANXA2 (A2) significantly increased trans-

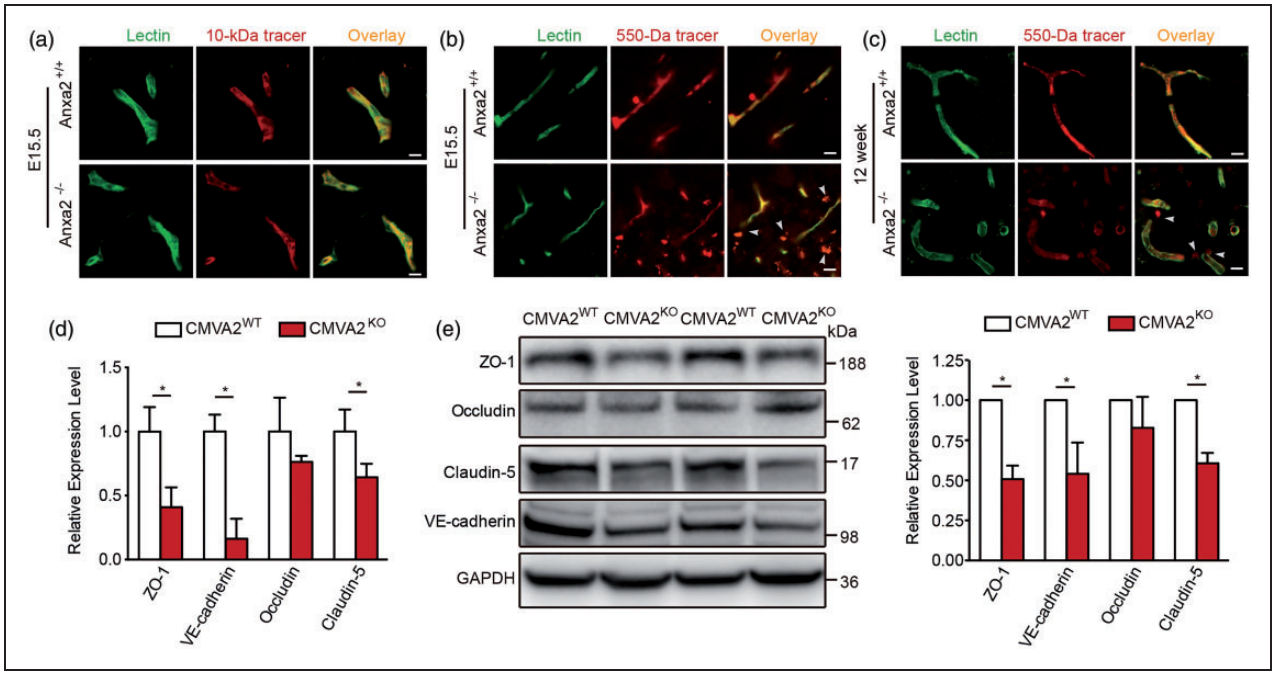

Figure 1. Annexin A2 (ANXA2) gene knockout impairs blood–brain barrier integrity. (a) Representative images of dorsal cortical plates from injected embryos after microvessels labeling with lectin (green) and 10 kDa dextran tracer (red). At E15.5 days, the tracer was primarily restricted to microvessels in both wild-type ($Anxa2^{+/+}$), and ANXA2 knock out ($Anxa2^{-/-}$) mice. (b) At E15.5 days, the smaller tracer sulfo-NHS-biotin (~550 Da) leaked out of microvessels in $Anxa2^{-/-}$ mice (arrowheads). (c) The sulfo-NHS-biotin was confined to microvessels in wild-type controls at 12 weeks, whereas it leaked out of the microvessels (arrowheads) in $Anxa2^{-/-}$ mice. $n = 5$ embryos or mice, bar = 25 μm. (d) Real-time polymerase chain reaction quantification of ZO-1, occludin, claudin-5, and VE-cadherin mRNA levels of isolated cerebral microvessel (CMV) fragments in 10–12 weeks old male $Anxa2^{+/+}$ ($CMVA2^{WT}$) and $Anxa2^{-/-}$ ($CMVA2^{KO}$) mice. $n = 6$ per group ($^*P < 0.05$, unpaired Student's *t*-test). (e) Representative western blot images and quantification of ZO-1, occludin, claudin-5, and VE-cadherin protein levels of isolated CMV fragments in 10–12 weeks old male $Anxa2^{+/+}$ ($CMVA2^{WT}$) and $Anxa2^{-/-}$ ($CMVA2^{KO}$) mice. $n = 6$ per group ($^*P < 0.05$, unpaired Student's *t*-test).

endothelial permeability, even at baseline (Figure 2(b)). Because cytokine-induced neuroinflammation is a major pathway that contributes to BBB dysfunction, we mimicked these in vivo scenarios by exposing HBMVEC to IL-1β (20 ng/ml). As expected, IL-1β stimulation induced an increase in trans-endothelial permeability (Figure 2(c)). Treatment with exogenous rA2 showed a dose-dependent rescue of permeability (Figure 2(c)). Besides inflammation, hypoxia-related pathways represent another major contributor to BBB leakage. Hence, we exposed HBMVEC to 24 h of hypoxic stress and measured the effects of rA2 on trans-endothelial permeability. As expected, hypoxia led to an increase in permeability and rA2 treatment was able to rescue these disruptions (Figure 2(d)). Finally, we tested the efficacy of rA2 in a combination insult experiment where endothelial cells were subjected to both 24 h hypoxia plus 20 ng/ml of IL-1β. The hypoxia plus IL-1β insult only slightly decreased cell number, but the changes were not significant (cell counting, data not shown). However, the combined hypoxia plus IL-1β insult clearly increased trans-endothelial permeability, and rA2 treatment significantly restored endothelial tightness (Figure 2(e) to (g)).

Role of ANXA2 in the regulation of junctional proteins after hypoxia plus IL-1β insult

Since junctional proteins are essential for maintaining endothelial tightness, we further explored the effects of rA2 on the expression and distribution of tight junction proteins (ZO-1, claudin-5, occludin) and the adherens junction protein VE-cadherin. Using total cell lysates and membrane fractions, we found that the expression of junctional proteins was significantly reduced after hypoxia plus IL-1β insult (Figure 3(a) and (b)). rA2 appeared to ameliorate these damaging effects by upregulating the total expression of junctional proteins (Figure 3(a)). rA2 also increased the amount of ZO-1 and VE-cadherin associated with membrane fractions (Figure 3(b)), although no changes were noted for occludin and claudin-5 (Figure 3(b)). Concordant with western blot results, immunostaining suggested that rA2 may promote the association of ZO-1 and

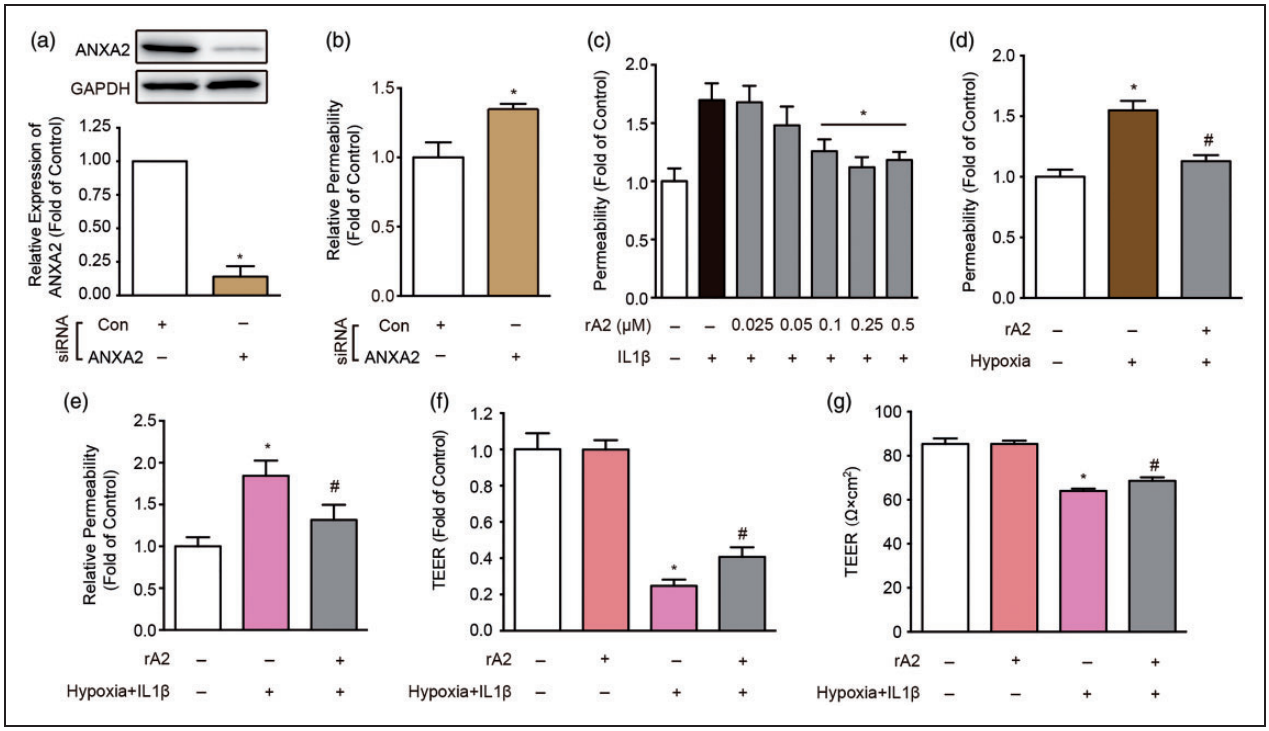

Figure 2. Role of annexin A2 (ANXA2) in the regulation of trans-endothelial permeability after hypoxia plus IL-1β insult. (a) ANXA2 expression in ANXA2 (A2) and control (Con) short interfering RNA (siRNA) transfected human brain microvascular endothelial cell cultures. $n = 6$ independent experiments ($^*P < 0.05$, unpaired Student's *t*-test). (b) Effect of ANXA2 (A2) and control (Con) siRNA on trans-endothelial permeability. $n = 5$ independent experiments ($^*P < 0.05$, unpaired Student's *t*-test). (c) The effects of recombinant ANXA2 (rA2) dose range in 24 h exposure of IL-1β (20 ng/ml)-induced trans-endothelial permeability increase. $n = 5$ independent experiments ($^*P < 0.05$ vs. IL-1β group, one-way analysis of variance (ANOVA) followed by Tukey's tests). (d) The effect of 100 nM rA2 in 24 h hypoxia-induced trans-endothelial permeability increase. $n = 5$ independent experiments ($^*P < 0.05$ vs. control, $^{\#}P < 0.05$ vs. hypoxia group, one-way ANOVA followed by Tukey's tests). (e) rA2 (100 nM) effects in IL-1β (20 ng/ml) plus hypoxia-induced trans-endothelial permeability increase. (f, g) rA2 (100 nM) effects in IL-1β (20 ng/ml) plus hypoxia-induced (f) relative and (g) absolute trans-endothelial electrical resistance (TEER) decrease. $n = 3$ independent experiments ($^*P < 0.05$ vs. control, $^{\#}P < 0.05$ vs. hypoxia + IL-1β group, one-way ANOVA followed by Tukey's tests).

VE-cadherin signals with the cell membrane outline (Figure 3(c) and (d)).

Interactions between ANXA2, VE-cadherin, and F-actin after hypoxia plus IL-1β insult

In epithelial cells and human umbilical vein endothelial cells, ANXA2 has been reported to bind VE-cadherin and F-actin.[8,26] To determine whether analogous interactions occur in brain endothelial cells, we performed immunoprecipitation experiments. Endogenous ANXA2 appeared to bind with VE-cadherin but not with ZO-1, claudin-5, and occludin (Figure 4(a) and (b)). For cytoskeleton, endogenous ANXA2 also showed a strong interaction with F-actin (Figure 4(a) and (c)). Since endogenous ANXA2 can interact with VE-cadherin and F-actin under baseline conditions, we proposed that hypoxia plus IL-1β insult might disrupt these membrane associations. Although the total expression of ANXA2 was not changed by hypoxia plus IL-1β (Figure 4(d)), the association of ANXA2 with membrane fractions was decreased (Figure 4(e)). Consistent with these western blot results, immunocytochemistry suggested that hypoxia plus IL-1β appeared to reduce the association of ANXA2 and VE-cadherin signals (Figure 4(f) and (h)), and treatment with exogenous ANXA2 seemed to restore this interaction (Figure 4(f) and (h)). A similar trend was observed between ANXA2 and F-actin (Figure 4(g) and (h)). Overall, these imaging data suggest an association of signals may be present between ANXA2, VE-cadherin, and F-actin although these experiments cannot provide causal proof of mechanistic interactions.

ANXA2 is a Robo4 ligand and modulates Robo4-paxillin-ARF6 signaling

Recent studies suggest that Robo4-paxillin-ARF6 signaling may be a key regulator of vascular stability.[27] Therefore, we asked whether this pathway is involved

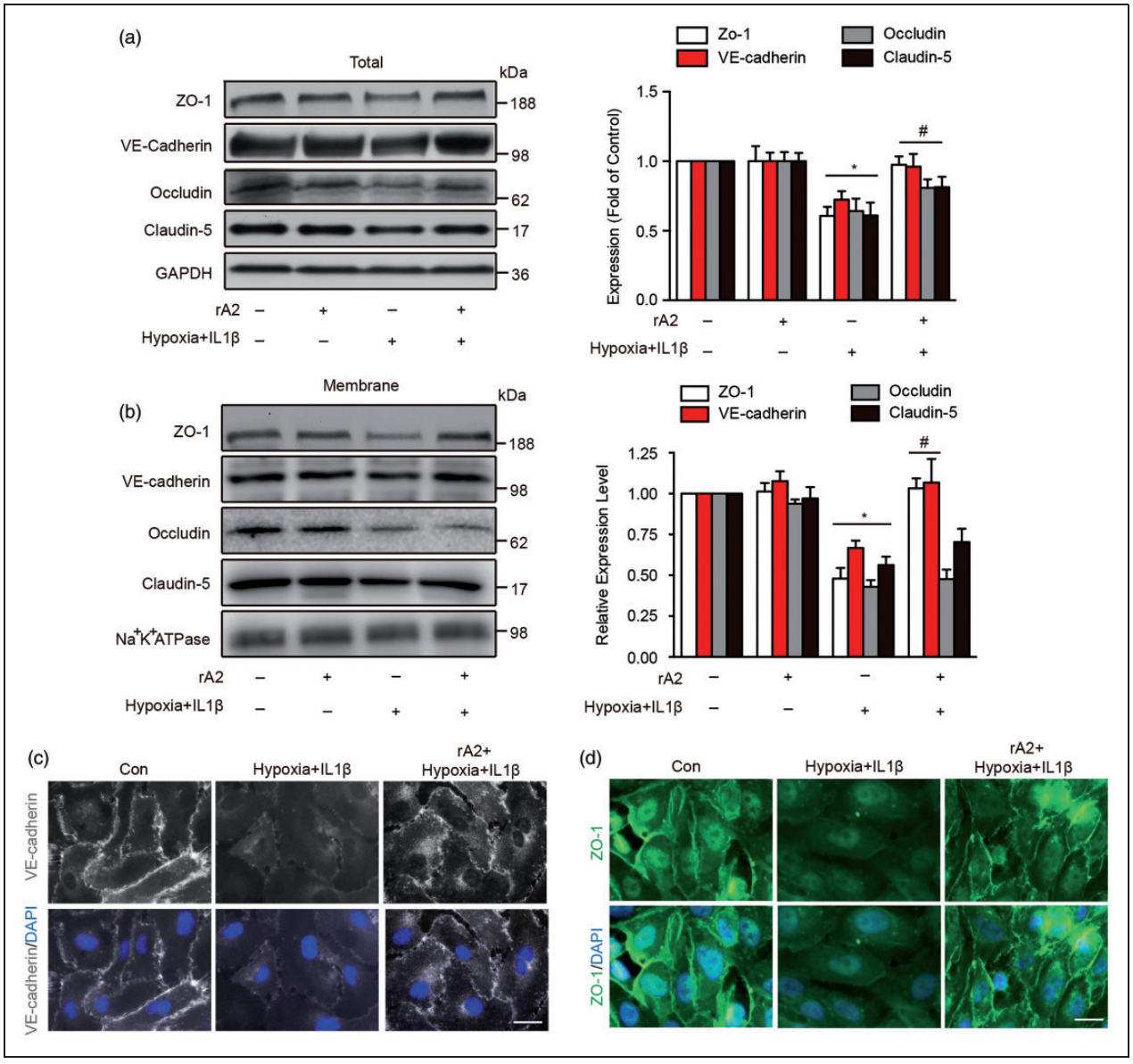

Figure 3. Role of annexin A2 in the regulation of junctional proteins after hypoxia plus IL-1β insult. (a) Gel images and quantification of western blots for ZO-1, occludin, claudin-5, and VE-cadherin expressions in total cell lysates. $n = 4$ independent experiments ($^{*}P < 0.05$ vs. control, $^{\#}P < 0.05$ vs. hypoxia + IL-1β group, two-way analysis of variance (ANOVA) followed by Bonferroni's tests). (b) Gel images and quantification of western blots for ZO-1, occludin, claudin-5, and VE-cadherin expressions on human brain microvascular endothelial cell membrane. $Na^{+}K^{+}$ATPase served as an equal loading control of cell membrane protein. $n = 4$ independent experiments ($^{*}P < 0.05$ vs. control, $^{\#}p < 0.05$ vs. hypoxia + IL-1β group, two-way ANOVA followed by Bonferroni's tests). (c) Immunocytochemistry of VE-cadherin. Bar = 25 μm, $n = 4$ independent experiments. (d) Immunocytochemistry of ZO-1. Bar = 25 μm, $n = 4$ independent experiments.

in our model system. Immunoprecipitation experiments demonstrated that ANXA2 was indeed able to bind to Robo4 but not to the related protein paxillin (Figure 5(a)). In our model system, siRNA suppression of ANXA2 decreased endogenous paxillin binding to Robo4, thus suggesting ANXA2 might be another vital endothelial membrane protein that modulates the interaction between Robo4 and paxillin (Figure 5(b)). After exposure to combined hypoxia plus IL-1β, Robo4-paxillin binding was similarly perturbed in the HBMVEC. Treatment with exogenous rA2 appeared to restore Robo4-paxillin interaction (Figure 5(c)). To test the effect of ANXA2 on ARF6 activation, HBMVEC were treated with ANXA2 siRNA. Silencing of ANXA2 significantly enhanced ARF6 activation (Figure 5(d)). Treatment of HBMVEC with IL-1β or combined hypoxia plus IL-1β led to an activation of ARF6 (Figure 5(e) and (f)). Notably, rA2 inhibited

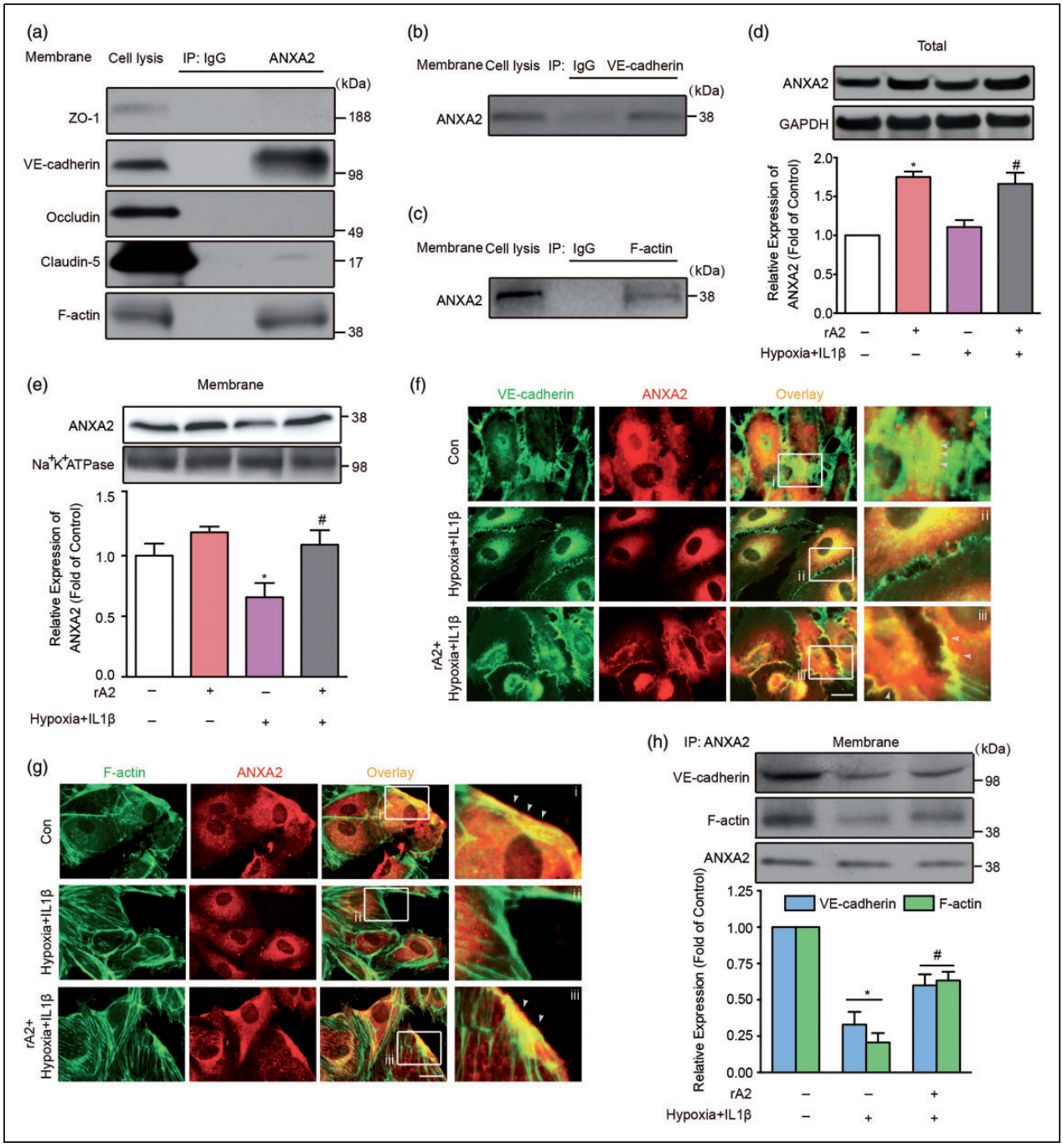

Figure 4. Interactions between annexin A2 (ANXA2), VE-cadherin, and F-actin after hypoxia plus IL-1β insult. (a–c) Immunoprecipitation (IP) and followed by immunoblotting of cell membrane lysates under normal condition, $n = 3$ independent experiments. (d) Gel images and quantification of western blots for ANXA2 expression in total cell lysates. $n = 4$ independent experiments ($^{*}P < 0.05$ vs. control, $^{\#}P < 0.05$ vs. hypoxia + IL-1β group, one-way analysis of variance (ANOVA) followed by Tukey's tests). (e) Gel images and quantification of western blots for ANXA2 expression in isolated human brain microvascular endothelial cell (HBMVEC) membrane. $n = 4$ independent experiments ($^{*}P < 0.05$ vs. control, $^{\#}P < 0.05$ vs. hypoxia + IL-1β group, one-way ANOVA followed by Tukey's tests). (f) Immunocytochemistry of ANXA2 and VE-cadherin. The zoomed regions from white boxes are shown alongside. White arrows indicate the association of signals between ANXA2 and VE-cadherin on HBMVEC membrane. Bar = 10 μm, $n = 3$ independent experiments. (g) Immunocytochemistry of ANXA2 and F-actin. The zoomed regions from white boxes are shown alongside. White arrows indicate the association of signals between ANXA2 and F-actin on HBMVEC membrane. Bar = 10 μm, $n = 3$ independent experiments. (h) Immunoprecipitation (IP) and followed by immunoblotting and quantification of isolated HBMVEC membrane after hypoxia plus IL-1β insult and recombinant ANXA2 treatment. $n = 4$ independent experiments ($^{*}P < 0.05$ vs. control, $^{\#}P < 0.05$ vs. hypoxia + IL-1β group two-way ANOVA followed by Bonferroni's tests).

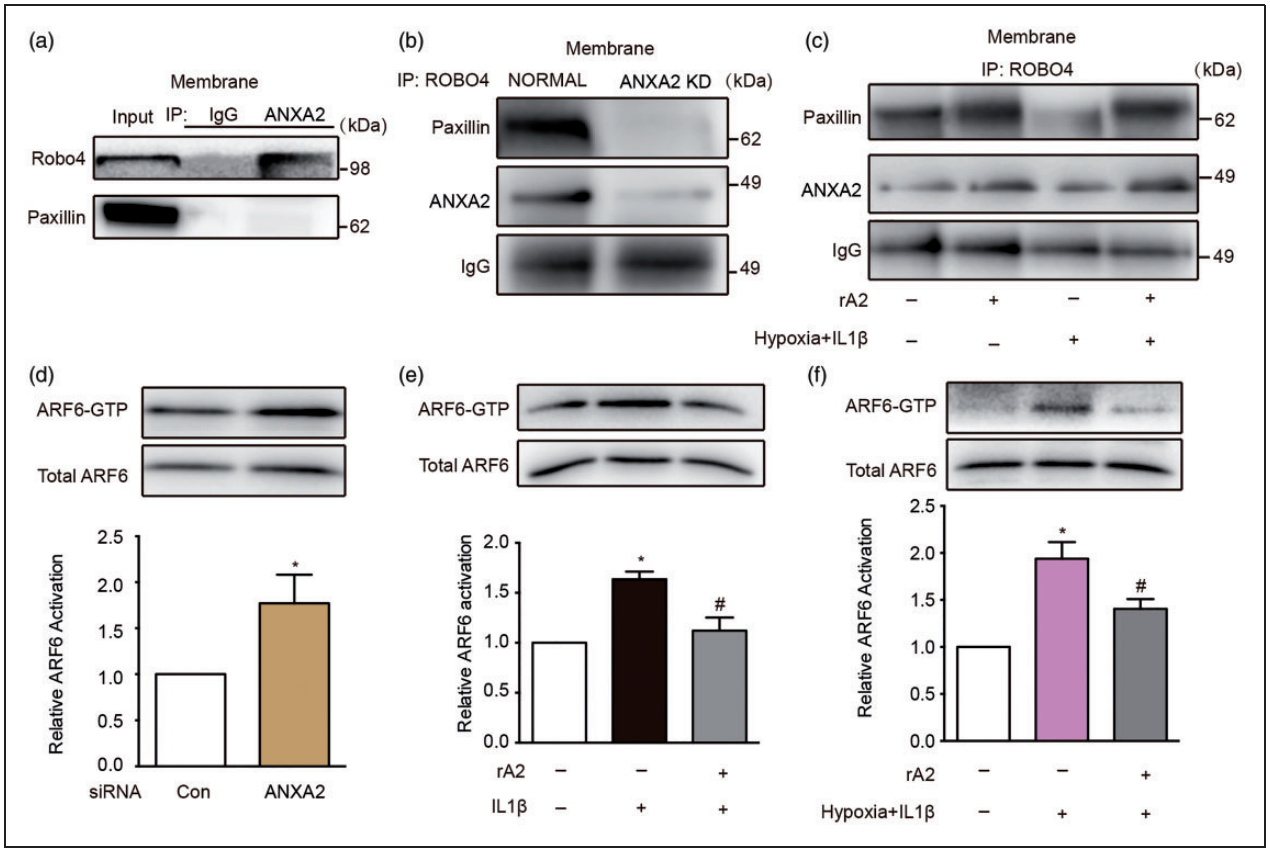

Figure 5. Annexin A2 (ANXA2) is a Robo4 ligand and modulates Robo4-paxillin-ADP-ribosylation factor 6 (ARF6) signaling. (a) Immunoprecipitation (IP) of isolated human brain microvascular endothelial cell (HBMVEC) membrane with anti-ANXA2 (A2) followed by immunoblotting with anti-Robo4 and anti-paxillin, $n = 3$ independent experiments. (b) Immunoprecipitation (IP) of isolated HBMVEC membrane with anti-Robo4 followed by immunoblotting with anti-ANXA2 and anti-paxillin under normal and ANXA2 knockdown (A2 KD) conditions, $n = 3$ independent experiments. (c) Immunoprecipitation (IP) of isolated HBMVEC membrane with anti-Robo4 followed by immunoblotting with anti-paxillin and anti-ANXA2 under hypoxia plus IL-1β insult with/without recombinant ANXA2 (rA2) treatment, $n = 3$ independent experiments. (d) The effect of control (Con) and ANXA2 short interfering RNA in ARF6 activation assessed by precipitation of ARF6-GTP (guanosine-5′-triphosphate) and quantification of the activated ARF6 levels by western blots. $n = 4$ independent experiments ($^{*}P < 0.05$, unpaired Student's *t*-test). (e) The effect of rA2 in IL-1β-induced ARF6 activation elevation. $n = 4$ independent experiments ($^{*}P < 0.05$ vs. control, $^{\#}P < 0.05$ vs. IL-1β group, one-way analysis of variance (ANOVA) followed by Tukey's tests). (f) The effect of rA2 in hypoxia plus IL-1β-induced ARF6 activation elevation. $n = 4$ independent experiments ($^{*}P < 0.05$ vs. control, $^{\#}P < 0.05$ vs. hypoxia + IL-1β group, one-way ANOVA followed by Tukey's tests).

IL-1β or combined hypoxia plus IL-1β-induced ARF6–GTP (Figure 5(e) and (f)).

rA2 modulates junctional proteins by inhibiting ARF6 activation

Activated ARF6 can suppress the expression of VE-cadherin on endothelial membranes.[24] So, we asked whether expression of other junctional proteins may also be mediated by ARF6. Treatment of HBMVEC with QS11, a potent agonist of ARF6, downregulated tight junctions and VE-cadherin mRNA expression in a dose-dependent manner (Figure 6(a)). Accordingly, treatment with SecinH3, an ARF6 inhibitor, significantly ameliorated the increase in trans-endothelial permeability after hypoxia plus IL-1β insults (Figure 6(b)).[28] Adding exogenous rA2 partially ameliorated ARF6 activation-induced reductions in ZO-1 and VE-cadherin (Figure 6(c)). Furthermore, inhibiting ARF6 with SecinH3 blocked the hypoxia plus IL-1β-induced increase in cell permeability, the downregulation of junctional proteins and association of these signals with cell membrane outlines (Figure 6(d) to (g)). Combination treatments with SecinH3 and rA2 appeared to lead to a better protective effect on cell permeability, junctional protein expression, and cell membrane association (Figure 6(d) to (g)). Collectively, these observations suggest that ANXA2 may be involved in the regulation of junctional proteins and trans-endothelial permeability by interacting with

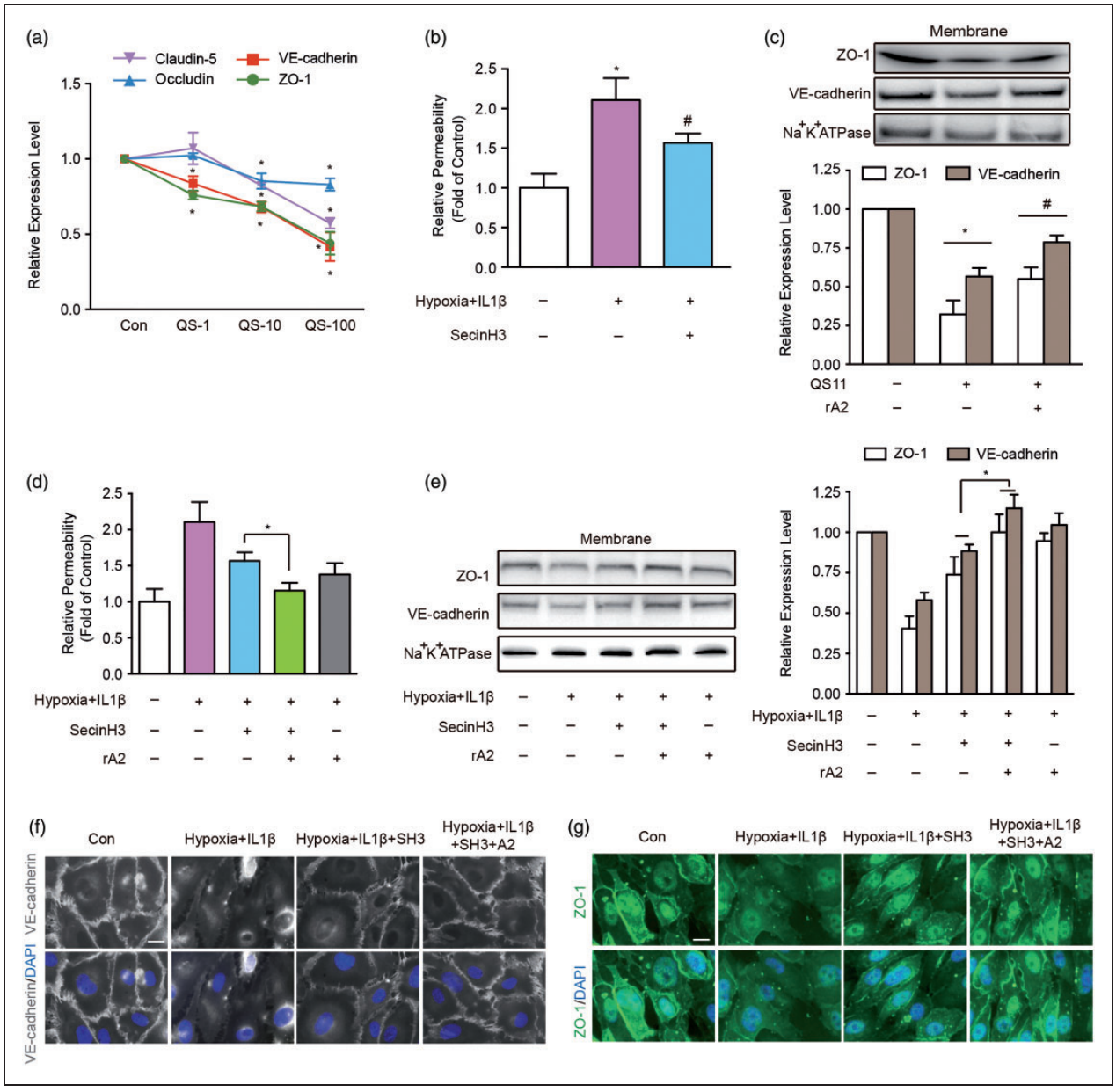

Figure 6. Recombinant ANXA2 (rA2) modulates junctional proteins by inhibiting ADP-ribosylation factor 6 (ARF6) activation. (a) Dose range effects of ARF6 specific agonist QS11 at 1 μM (QS-1), 10 μM (QS-10), and 100 μM (QS-100) on ZO-1, occludin, claudin-5, and VE-cadherin mRNA expression quantified by RT-PCR at 6 h after QS11 exposure to the human brain microvascular endothelial cells (HBMVEC). $n = 4$ independent experiments ($^*P < 0.05$ vs. control, two-way analysis of variance (ANOVA) followed by Bonferroni's tests). (b) The effect of the ARF6 inhibitor SecinH3 in trans-endothelial permeability. $n = 4$ independent experiments ($^*P < 0.05$ vs. control, $^{\#}P < 0.05$ vs. hypoxia + IL-1β group, one-way ANOVA followed by Tukey's tests). (c) Representative western blot gel images and quantification of ZO-1 and VE-cadherin protein expression in isolated HBMVEC membrane under resting physiological condition. $n = 3$ independent experiments ($^*P < 0.05$ vs. control, $^{\#}P < 0.05$ vs. QS11 group, two-way ANOVA followed by Bonferroni's tests). (d) The effect of the ARF6 inhibitor SecinH3 or/and rA2 in hypoxia plus IL-1β-induced trans-endothelial permeability. $n = 3$ independent experiments ($^*P < 0.05$ one-way ANOVA followed by Tukey's tests). (e) Representative western blot gel images and quantification of ZO-1 and VE-cadherin protein expressions in isolated HBMVEC membrane. $n = 4$ independent experiments ($^*P < 0.05$, two-way ANOVA followed by Bonferroni's tests). (f) Immunocytochemistry of VE-cadherin. Bar = 25 μm, $n = 3$ independent experiments. (g) Immunocytochemistry of ZO-1. Bar = 25 μm, $n = 3$ independent experiments.

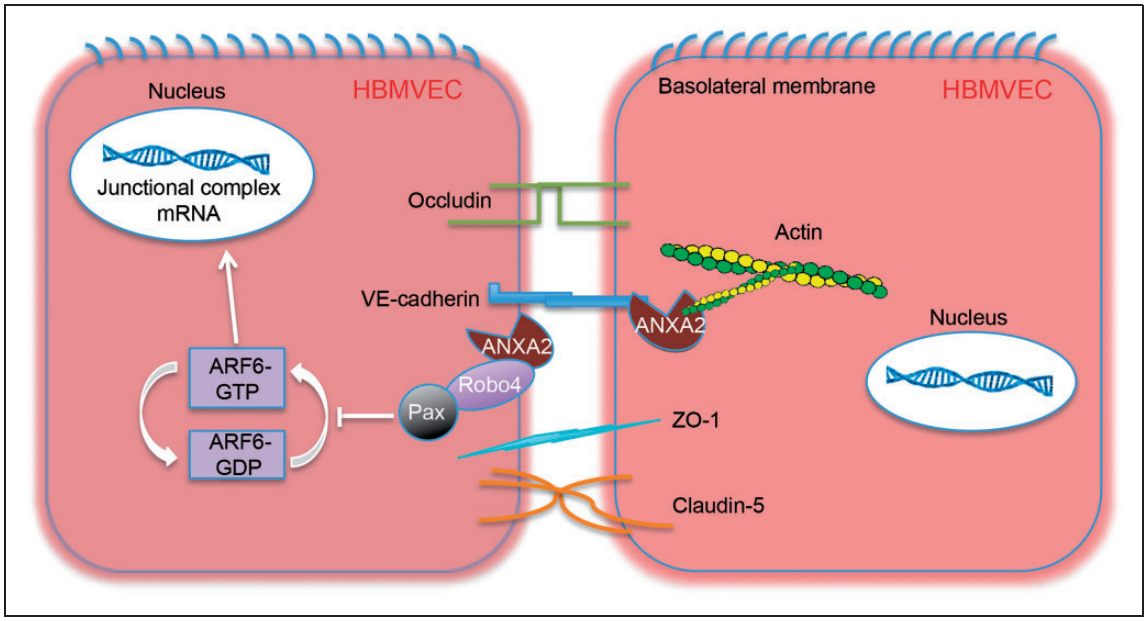

Figure 7. Working model of the role of annexin A2 (ANXA2) in cerebral trans-endothelial integrity. ANXA2 appears to interact extracellularly and intracellularly with VE-cadherin, F-actin, and regulate Robo4-paxillin-ADP-ribosylation factor 6 (ARF6) pathway. The data presented in this study evoke a model for trans-endothelial permeability protection by ANXA2. Endothelial cell membrane protein ANXA2 and exogenous recombinant ANXA2 can interact with junctional complexes, such as VE-cadherin and F-actin, which stabilize their intercellular junction structures. Moreover, we discovered the interaction between ANXA2 and Robo4 on the cell membrane, which may enhance the Robo4-paxillin (Pax) association, leading to inhibition of ARF6 activation (inactive ARF6-GDP (guanosine-diphosphate) converts to active ARF6-GTP (guanosine-5′-triphosphate)) and associated downregulation of junctional proteins expression.

VE-cadherin/F-actin and mediating Robo4-paxillin-ARF6 pathway.

Discussion

In the first set of experiments, by using *Anxa2*$^{-/-}$ mice, we showed for the first time that ANXA2 is an essential membrane protein that contributes to BBB development. Increased BBB leakage of a small molecule tracer in E15.5 embryos and adult (3-month-old male) mice compared to WT mice indicates that the BBB still forms, albeit more slowly and less tightly, in the absence of ANXA2. Furthermore, depletion of ANXA2 gene decreases tight junction proteins ZO-1, Claudin-5, and adherens junction protein VE-cadherin in isolated CMV fragments, suggesting that the unique role of ANXA2 in BBB formation and function may involve the regulation of these cell-to-cell junctions.

In the second set of experiments, we used cell culture injury models to demonstrate that (1) endogenous cell membrane protein ANXA2 plays an important role in maintaining trans-endothelial tightness in HBMVEC, (2) ANXA2 associates with cell membrane F-actin and VE-cadherin, (3) cell membrane ANXA2 is a ligand of Robo4, (4) exogenous rA2 can ameliorate hypoxia plus IL-1β-induced changes in trans-endothelial permeability, and (5) these protective effects of rA2 are mediated in part via F-actin/VE-cadherin interactions to strengthen endothelial tightness, as well as the ability of rA2 to modulate Robo4-paxillin-ARF6 signaling pathway and deactivate ARF6.

ANXA2 is a multifunctional protein that belongs to a large family of Ca^{2+}-dependent anionic phospholipid and membrane-binding proteins. Emerging evidence suggests that ANXA2 plays a vital role in vascular homeostasis, including regulation of cell surface fibrinolysis and angiogenesis.[29,30] Previous investigations have found ANXA2 can bind to VE-cadherin and F-actin in epithelial cells and human umbilical vein endothelial cells.[8–10,26] ANXA2 can be expressed in brain endothelium as well,[29,31] but it was not known whether these ANXA2 binding properties might also help control junctional proteins in the brain. Here, we showed that ANXA2 could indeed play a role in regulating cerebral endothelial junctions in part by promoting F-actin and VE-cadherin interactions (Figure 7), and importantly, these pathways may be important for BBB development as well the protection of trans-endothelial tightness after injury.

In addition to ANXA2 interactions with cytoskeletal elements, our study also suggests a role for Robo4-paxillin-ARF6 signaling (Figure 7), a pathway that has been previously proposed as a key regulator of

vascular stability.[24,27] ARF6 is known to suppress the expression of VE-cadherin and augment VEGF signaling to increase endothelial permeability.[32,33] Formation of a Robo4-paxillin complex on the cell membrane can block the activation of ARF6, thereby increasing endothelial tightness and integrity. Our results showed for the first time that ANXA2 binds Robo4 and this contributes to the formation of Robo4-paxillin complex, thus blocking ARF6 and reducing endothelial permeability. From a translational perspective, these pathways may be important for potential therapeutic applications. Treating HBMVEC with the ARF6 activator QS11 or inhibitor SecinH3 significantly decreased or increased junctional proteins expression, respectively. Exogenous recombinant ANXA2, that is, rA2, can also bind to Robo4 and prevent hypoxia plus IL-1β-induced dissociation of Robo4-paxillin, thus, blocking ARF6 activation and ameliorating the downregulation of junctional proteins and preserving endothelial tightness. These findings suggest that rA2-related pathways may represent a potentially novel approach to rescue BBB function by directly modulating the signaling and regulatory pathways of junctional homeostasis in the cerebral endothelium.

Nevertheless, we are aware that several mechanistic caveats may exist. First, our in vivo experiments here only provide a starting point. Deeper studies are warranted to investigate how ANXA2 may interact with other more well-characterized signals and substrates during BBB development. Second, our in vitro ANXA2-Robo4 signaling data are primarily focused on endothelial permeability. However, Robo-mediated mechanisms are also important for angiogenesis. Future studies should carefully examine whether and how the targeting of ANXA2 pathways may influence vascular growth and remodeling after injury. Third, it appears that exogenous rA2 may also stimulate endogenous ANXA2 responses, at least within the context of our cell model systems. How these positive feedback loops may affect the aggregate endothelial response remains to be determined. Finally, we used hypoxia plus IL-1β to mimic two major triggers of cerebrovascular injury and leakage. However, brain pathophysiology is complex and multifactorial, so a perfect in vitro BBB model may not exist.[34,35] Beyond endothelial permeability per se, it will be useful to ask how ANXA2 signaling may affect other key aspects of the BBB including transporters, matrix proteases, and cell–cell signaling at the neurovascular interface.

In summary, our data suggest that ANXA2 plays an important role in regulating cerebral endothelial permeability via F-actin–VE-cadherin interactions and Robo4-paxillin-ARF6 signaling (Figure 7). Further translational studies are warranted to explore the relevance of ANXA2-related pathways as a therapeutic target for protecting the BBB and cerebrovascular integrity in neurological disease.

Funding

The author(s) disclosed receipt of the following financial support for the research, authorship, and/or publication of this article: This work was supported by National Institutes of Health (NIH) grants (RO1 NS092085 to XW and R01 HL042483 to KAH); Natural Science Foundation of China (NSFC) grants (81703498 to WL; 81773700, 81373391, and 81573402 to HD).

Acknowledgements

We thank J. Lok for her very helpful discussion from the clinical translation perspective.

Declaration of conflicting interests

The author(s) declared no potential conflicts of interest with respect to the research, authorship, and/or publication of this article.

Authors' contributions

WL and ZC designed and executed most of the experiments. ZY, JY, CC, and QZ performed part of experiments and data analysis. KH helped in the experimental design and result interpretation. HD, ZC, EL, and XW designed experiments, interpreted the data, and wrote the manuscript. LH helped with manuscript editing.

Supplementary material

Supplementary material for this paper can be found at the journal website: http://journals.sagepub.com/home/jcb

References

1. Hawkins BT and Davis TP. The blood–brain barrier/neurovascular unit in health and disease. *Pharmacol Rev* 2005; 57: 173–185.
2. Neuwelt EA, Bauer B, Fahlke C, et al. Engaging neuroscience to advance translational research in brain barrier biology. *Nat Rev Neurosci* 2011; 12: 169–182.
3. Banks WA. From blood–brain barrier to blood–brain interface: new opportunities for CNS drug delivery. *Nat Rev Drug Discov* 2016; 15: 275–292.
4. Erdo F, Denes L and de Lange E. Age-associated physiological and pathological changes at the blood–brain barrier: a review. *J Cereb Blood Flow Metab* 2017; 37: 4–24.
5. Na W, Shin JY, Lee JY, et al. Dexamethasone suppresses JMJD3 gene activation via a putative negative glucocorticoid response element and maintains integrity of tight junctions in brain microvascular endothelial cells. *J Cereb Blood Flow Metab* 2017; 37: 3695–3708.
6. Li W, Chen Z, Chin I, et al. The role of VE-cadherin in blood-brain barrier integrity under central nervous system pathological conditions. *Curr Neuropharmacol*. Epub ahead of print 22 February 2018. doi: 10.2174/1570159X16666180222164809.

7. Bharadwaj A, Bydoun M, Holloway R, et al. Annexin A2 heterotetramer: structure and function. *Int J Mol Sci* 2013; 14: 6259–6305.
8. Heyraud S, Jaquinod M, Durmort C, et al. Contribution of annexin 2 to the architecture of mature endothelial adherens junctions. *Mol Cell Biol* 2008; 28: 1657–1668.
9. Su SC, Maxwell SA and Bayless KJ. Annexin 2 regulates endothelial morphogenesis by controlling AKT activation and junctional integrity. *J Biol Chem* 2010; 285: 40624–40634.
10. Lee DB, Jamgotchian N, Allen SG, et al. Annexin A2 heterotetramer: role in tight junction assembly. *Am J Physiol Renal Physiol* 2004; 287: F481–F491.
11. Luo M, Flood EC, Almeida D, et al. Annexin A2 supports pulmonary microvascular integrity by linking vascular endothelial cadherin and protein tyrosine phosphatases. *J Exp Med* 2017; 214: 2535–2545.
12. Ben-Zvi A, Lacoste B, Kur E, et al. Mfsd2a is critical for the formation and function of the blood–brain barrier. *Nature* 2014; 509: 507–511.
13. Ek CJ, Dziegielewska KM, Stolp H, et al. Functional effectiveness of the blood–brain barrier to small water-soluble molecules in developing and adult opossum (*Monodelphis domestica*). *J Comp Neurol* 2006; 496: 13–26.
14. Ling Q, Jacovina AT, Deora A, et al. Annexin II regulates fibrin homeostasis and neoangiogenesis in vivo. *J Clin Invest* 2004; 113: 38–48.
15. Zhu H, Fan X, Yu Z, et al. Annexin A2 combined with low-dose tPA improves thrombolytic therapy in a rat model of focal embolic stroke. *J Cereb Blood Flow Metab* 2010; 30: 1137–1146.
16. Wang X, Lee SR, Arai K, et al. Lipoprotein receptor-mediated induction of matrix metalloproteinase by tissue plasminogen activator. *Nat Med* 2003; 9: 1313–1317.
17. Lin L, Wang Q, Qian K, et al. bFGF protects against oxygen glucose deprivation/reoxygenation-induced endothelial monolayer permeability via S1PR1-dependent mechanisms. *Mol Neurobiol* 2018; 55: 3131–3142.
18. Shindo A, Maki T, Mandeville ET, et al. Astrocyte-derived pentraxin 3 supports blood–brain barrier integrity under acute phase of stroke. *Stroke* 2016; 47: 1094–1100.
19. Dimitrijevic OB, Stamatovic SM, Keep RF, et al. Effects of the chemokine CCL2 on blood–brain barrier permeability during ischemia-reperfusion injury. *J Cereb Blood Flow Metab* 2006; 26: 797–810.
20. Wang Q, Yuan J, Yu Z, et al. FGF21 Attenuates High-Fat Diet-Induced Cognitive Impairment via Metabolic Regulation and Anti-inflammation of obese mice. *Mol Neurobiol* 2017; 55: 4702–4717.
21. Du Y, Deng W, Wang Z, et al. Differential subnetwork of chemokines/cytokines in human, mouse, and rat brain cells after oxygen-glucose deprivation. *J Cereb Blood Flow Metab* 2017; 37: 1425–1434.
22. Hayakawa K, Pham LD, Seo JH, et al. CD200 restrains macrophage attack on oligodendrocyte precursors via toll-like receptor 4 downregulation. *J Cereb Blood Flow Metab* 2016; 36: 781–793.
23. Choi YK, Maki T, Mandeville ET, et al. Dual effects of carbon monoxide on pericytes and neurogenesis in traumatic brain injury. *Nat Med* 2016; 22: 1335–1341.
24. Zhu W, London NR, Gibson CC, et al. Interleukin receptor activates a MYD88-ARNO-ARF6 cascade to disrupt vascular stability. *Nature* 2012; 492: 252–255.
25. Dong W, Zhang GN and Gao SH. Preliminary in vitro analysis of mechanism of cardiac microvascular endothelial barrier function. *Genet Mol Res* 2016; 15. DOI: 10.4238/gmr15048864.
26. Grieve AG, Moss SE and Hayes MJ. Annexin A2 at the interface of actin and membrane dynamics: a focus on its roles in endocytosis and cell polarization. *Int J Cell Biol* 2012; 2012: 852430.
27. Jones CA, Nishiya N, London NR, et al. Slit2-Robo4 signalling promotes vascular stability by blocking ARF6 activity. *Nat Cell Biol* 2009; 11: 1325–1331.
28. Hafner M, Schmitz A, Grune I, et al. Inhibition of cytohesins by SecinH3 leads to hepatic insulin resistance. *Nature* 2006; 444: 941–944.
29. Dai H, Yu Z, Fan X, et al. Dysfunction of annexin A2 contributes to hyperglycaemia-induced loss of human endothelial cell surface fibrinolytic activity. *Thromb Haemost* 2013; 109: 1070–1078.
30. Luo M and Hajjar KA. Annexin A2 system in human biology: cell surface and beyond. *Semin Thromb Hemost* 2013; 39: 338–346.
31. Kwaan HC, Wang J and Weiss I. Expression of receptors for plasminogen activators on endothelial cell surface depends on their origin. *J Thromb Haemost* 2004; 2: 306–312.
32. Klein S, Partisani M, Franco M, et al. EFA6 facilitates the assembly of the tight junction by coordinating an ARF6-dependent and -independent pathway. *J Biol Chem* 2008; 283: 30129–30138.
33. Zhu W, Shi DS, Winter JM, et al. Small GTPase ARF6 controls VEGFR2 trafficking and signaling in diabetic retinopathy. *J Clin Invest*. 2017; 127: 4569–4582.
34. Li Q, Han X and Wang J. Organotypic hippocampal slices as models for stroke and traumatic brain injury. *Mol Neurobiol* 2016; 53: 4226–4237.
35. Helms HC, Abbott NJ, Burek M, et al. In vitro models of the blood–brain barrier: an overview of commonly used brain endothelial cell culture models and guidelines for their use. *J Cereb Blood Flow Metab* 2016; 36: 862–890.